

Development of a Finite Element Model for W-Beam Guardrails

Background:

During the early 1960's a wide variety of guardrail systems were developed and installed on highways in the US. W-beam guardrails use steel sheets rolled into the W-shape to form a rigid beam that can "catch" the bumpers of typical vehicles. W-beam guardrails have become the most common type of longitudinal roadside barriers used on the roadways in the United States. They have played an important role in improving highway safety when used to redirect vehicles away from roadside hazards such as bridge abutments, light poles, trees, ditches, mounds, severe terrain, or other fixed objects found along the roadside.

Figure 1 shows the features of a typical w-beam guardrail barrier with steel posts and wood blockouts. As guardrail systems evolved, variations developed in posts, rail connections, blockouts, and other elements of the barrier. One significant change resulted from the implementation of the NCHRP Report 350 recommendations for the evaluation of roadside safety features [1]. Report 350 recommended a larger vehicle (the 2000 kg pick-up truck) for testing. This vehicle was considered more representative of the light truck utility vehicles on the road, but it was recognized that the added weight would increase the kinetic energy in crashes with roadside hardware.

Full-scale crash tests were conducted on w-beam guardrail systems to examine the performance of the G4(1s) guardrail system under the NCHRP Report 350 guidelines [2, 3,4]. The initial full-scale crash tests for Test Level 3 (TL 3) with a 2000 kg vehicle at a 100 km/h impact speed and a 25 degree impact angle showed that w-beam guardrails with steel blockouts did not meet the criteria of NCHRP Report 350. Subsequently, w-beam guardrails were tested with different types of posts and blockouts in attempts to find a viable design. Eventually, through traditional analysis and a series of trial and error crash tests, a cost effective means was found to retrofit the standard w-beam guardrail to meet the new crashworthiness criteria at TL 3. Full-scale crash testing ultimately determined that a design with steel posts and routed wood blockouts would meet the NCHRP 350 TL 3 criteria.

It became apparent in efforts to find an improved design for this guardrail system, that a better means to evaluate design variations was needed. This technical summary describes efforts to develop and demonstrate a viable alternative approach to addressing design improvement needs.



Figure 1 – Typical standard W-beam guardrail G4(1s).

Approach:

Crash simulations using finite element models had been emerging as a means to conduct detailed analyses of crash or impact events in other fields. The objective of this study was to develop a viable finite element (FE) model for the standard w-beam guardrail system and use it with an available FE vehicle model in crash simulations to investigate the effects of design variations on the safety performance of w-beam guardrail systems.

The study involved three steps. In the first step, a detailed finite element model of the guardrail system was created incorporating details of the rail, connections, the post, the blockout, and the soil in which the post was embedded. The second step involved validations of the model by comparisons of simulated results to data from previously conducted full-scale crash tests. The third step involved using the validated model as the basis for studying the effects of w-beam guardrail design variations.

In this analysis, the dynamic explicit finite element code LS-DYNA [5] was used to simulate the crash performance of w-beam guardrails in accordance with procedures for Test 3-11 in NCHRP Report 350. The LS-DYNA finite element analysis program uses an explicit LaGrangian numerical method to solve three-dimensional, dynamic, nonlinear, large displacement problems. While the software’s initial application was in military-related studies, in the past 15 years, LS-DYNA has gained new ground in automotive analysis such as crashworthiness and occupant safety. More recently, the code has been successfully used in analyzing other structures including roadside hardware [6, 7, 8].

Modeling Guardrail Components:

The Roadside Design Guide (RDG) designates the G4(1s) as a strong-post guardrail system. It uses a 12 gauge steel w-beam rail, mounted on steel posts spaced at 1.905m (6 ft 3 in) with a wood or steel blockout on each post to reduce the potential for an impacting vehicle to snag on the posts during impacts. The barrier has been found to have a maximum dynamic deflection of about 1m (3 ft) under TL 3 test conditions.

The finite element model of the w-beam guardrail system developed in this effort included detailed representations of all components to ensure that the model was an accurate representation of the actual system. First, the explicit geometry of all components was incorporated in the model (Figure 2). This included the w-beams, posts, blockouts, and bolts. This ensured that the correct mass, inertia, and stiffness of the different parts was reflected in the model.

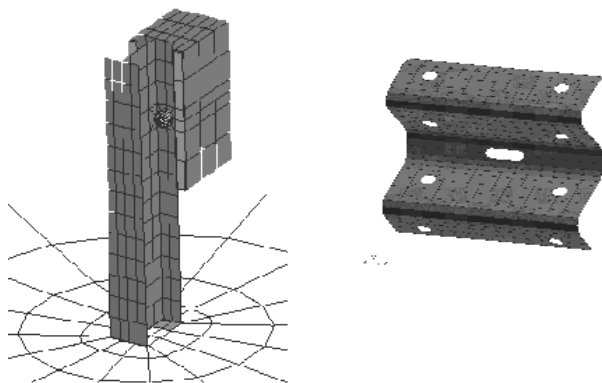


Figure 2 – Meshed representations of guardrail component geometry.

Modeling of Steel and Soil Elements

Appropriate material and cross-sectional properties were assigned to all components of the guardrail system. The metal components, such as the posts and

w-beams, were represented as piecewise, linear, plastic materials. Models of this material have been extensively utilized to represent structural metals and have been fully validated and optimized. The material behavior is isotropic, elasto-plastic with strain rate effects and failure. The properties used for these materials were extracted from the literature and determined empirically from coupon tests that were performed on similar steels.

The soil and foam model in LS DYNA was used to represent the soil. The properties used for this model were back-calculated from data obtained in impact tests of wood and steel posts embedded in specific types of soil. Simulations of these tests were performed and the material properties were varied until soil resistance and deformations predicted by the simulation matched the results of the prior impact tests.

Post & Blockout Elements

A detailed finite element model of the steel post with wooden blockout is shown in Figure 3. For computational purposes, six rails located at the middle of the full guardrail system were modeled using fine mesh while the remaining rails were modeled using coarser mesh. All posts and rails were modeled using quadrilateral shell elements. The shell element used in this analysis is based on the Belytschko-Lin-Tsay shell formulation [9]. Wooden blockouts were modeled using eight-node reduced integration hexahedral solid elements. These elements capture the behavior of the components at much less cost because they consume much less computer time and memory.

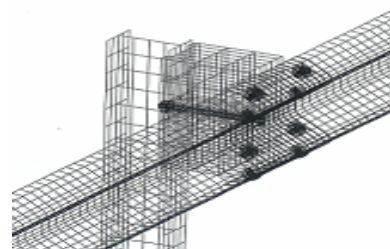


Figure 3 – Model of the guardrail, blockout, bolts, and post.

Bolt Modeling:

Eight small bolts are used to connect sections of w-beam together and a long bolt is used to connect the rails to the wooden blockout and post as shown in Figures 3 & 4. For the small bolts and nuts, a rigid material formulation was used. This assumption was

made to reduce the computation time since small elements are needed to capture the geometry of the bolts. A spring is placed between the bolt head and the nut to represent the stiffness of the bolt. The properties of these springs are determined from the material properties, cross-sectional area, and length of the bolt.

The long bolts have significant effect on the behavior of the G4(1s) system and have to be modeled in detail. To accurately and efficiently represent these bolts, a special modeling technique was utilized. In this technique, the bolt is modeled with beam elements to capture its tensile, bending, and shear behavior. By using beam elements, the time step is not controlled by the cross-sectional geometry of the bolt. Hence, a larger simulation time step and smaller computation time is needed to reach a solution. The elasto-plastic material model with failure was assigned to the beam elements to simulate the nonlinear and failure behavior of the bolt. The geometry of the bolt is represented by shell elements with “null” material properties. The null shell elements have no effect on the stiffness of the bolts and their size does not affect the simulation time step. They are used to represent the bolt geometry for contact purposes only. Nodes from the shell elements are tied to the beam element nodes to transfer the contact forces. This method has been successfully used in previous studies [6, 7, 8, 9] and was found to be very accurate and efficient.

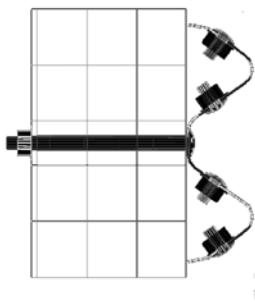


Figure 4 – Bolt details in the FE guardrail model.

Soil and Soil/Post Model

The soil was modeled as a cylindrical block 2.7m (9 ft) in diameter and 2.02m (6.5 ft) in length as shown in Figure 5. These dimensions were chosen such that the behavior of the soil and post/soil interaction is accurately captured with reasonable computation time. The outer boundaries of the soil model were constrained using the non-reflection boundary constraint option to prevent the stress wave from reflecting at the fixed boundary. The soil block is modeled using eight node hexahedral solid elements. The shape of the post was incorporated into the soil mesh with appropriate flange and web thickness to avoid penetration between post and soil and to have full representation of the post/soil

interaction. The automatic single surface sliding interface is defined between the outer faces of the post and inner faces of the soil block to simulate friction and the contact between the post and the soil.

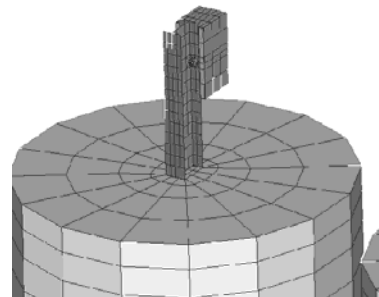


Figure 5 – Cylindrical soil block aspect of the model to allow analysis of soil-post interaction.

System Model

The guardrail system used in this study is based on the modified G4(1s) design. The rails are standard 12-gauge w-beams with lengths of 3.807 m (12.5ft) supported using W150x12.6 (W6x9) steel posts. These posts are 1830 mm (72in) length and embedded 1100 mm (43.3in) into the ground. Routed wood blockouts with dimensions of 150 mm x 200 mm x 360 mm (6 in x 8 in x 14 in) are placed between the posts and the w-beam rails. The system-level model of the G4(1s) guardrail system is modeled to have a total length of 53.3m (175 ft) and it is anchored at both ends using a standard Breakaway Cable Terminal (BCT). The system consists of 29 posts and 14 w-beam sections. Views of the model are provided in Figures 6 and 7.

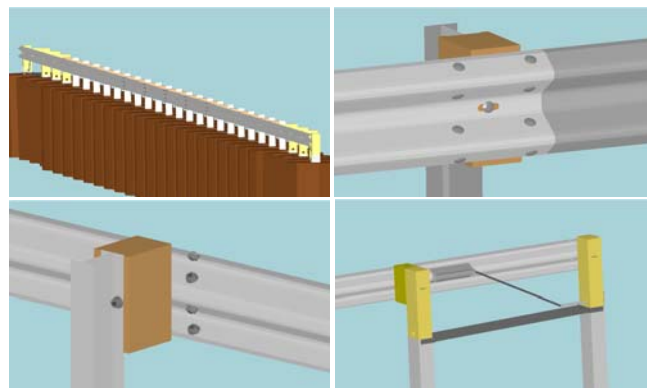


Figure 6 – Views of the components of the guardrail system model.

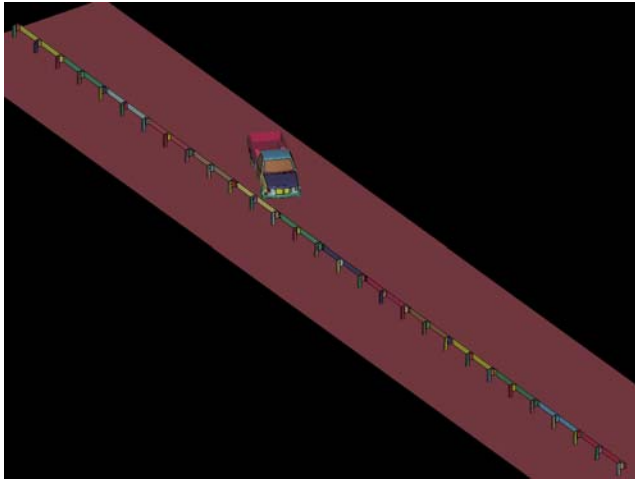


Figure 7 – Model set-up for vehicle-barrier impacts.

Model Validation:

A full-scale crash test, which had been performed at the Texas Transportation Institute, was selected for model validation. The conditions of this test were replicated in the individual guardrail and vehicle models. The initial crash simulation runs served to identify and correct deficiencies in the model. This process continued until reasonable correlations were obtained between the full-scale test data and simulation results. Figure 8 shows comparisons in a sequence of views between the simulation and test results at corresponding time steps in a crash event. These were judged to indicate that the model was effectively replicating the crash event.

The dynamic and permanent test article deflections reported in the crash test were compared to the results from the simulation (Table 1). The dynamic deflection is higher in the simulation than in the test while the permanent deformation is slightly lower. This difference was attributed to differences between the soil modeled for the simulations and the actual soil used in the crash test. Permanent deformation from the test and simulations are shown in Figure 9. Similarly, the occupant impact velocities and ridedown acceleration values from the simulation and from the crash test were satisfactorily compared. This led to the conclusion that the model was viable.

Table 1 – Comparison of dynamic and permanent deflections between crash test and simulation.

Deflection (m)	Crash Test	Simulation
Dynamic	1.0	1.23
Permanent	0.7	0.64

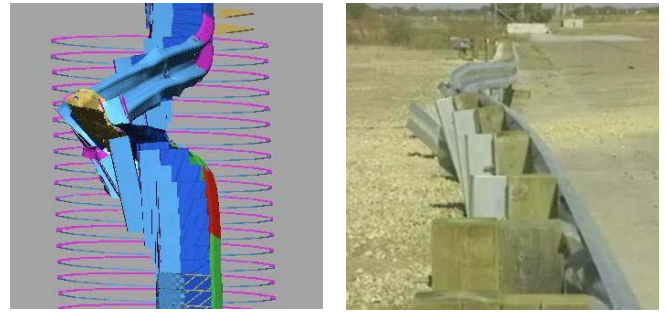


Figure 9 – Visual comparison of permanent barrier deflection from simulation and crash test.

Evaluating Design Alternatives:

The viability of a the use of modeling and crash simulation to evaluate guardrail design alternatives was demonstrated by the analysis of several design features, including:

- Routed versus non-routed blockouts.
- Varying rail steel gauge (12 versus 14 gauge).
- Blockout gap (0 mm versus 5 mm).

In the course of this research, the validated FE model was modified to reflect each of these changes and additional crash simulation runs executed. Some results from these analyses are described below.

Routed versus Non-Routed Blockouts

Simulation was used to compare routed versus non-routed blockouts [11] The comparison of roll angle recorded in crash tests and in simulation results is shown in Figure 10. Note that roll angles are greater (both test and simulation) for non-routed blockouts. A non-routed blockout bolted to the post was simulated as another means to stop the rotation of the blockout (dark purple line) It can be noted that the crash performance was similar relative to roll angle, but not as good for other measures.

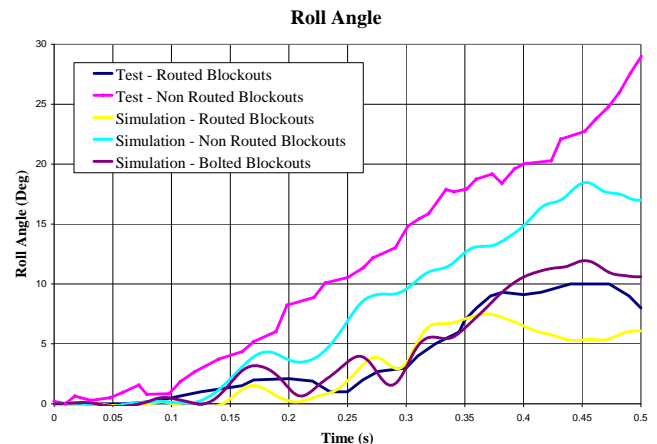


Figure 10 – Comparison of roll angle for various blockout designs.

12 Gauge versus 14 Gauge Rail Thickness

Similarly, simulation was used to evaluate differences in performance related to the gauge of the steel used for the w-beam rail. This analysis indicated that the thinner 14 gauge steel would effectively redirect a vehicle under TL3, but using the material strain information from the simulation showed that during impact the area around the splice reached its maximum load capacity (e.g., plastic strain). These regions are depicted in red in Figure 11. While the system could pass the NCHRP 350 requirements, the potential for strain failures at the splice increased. This was noted to be more likely when corrosion or minor damage to the rail occurred.

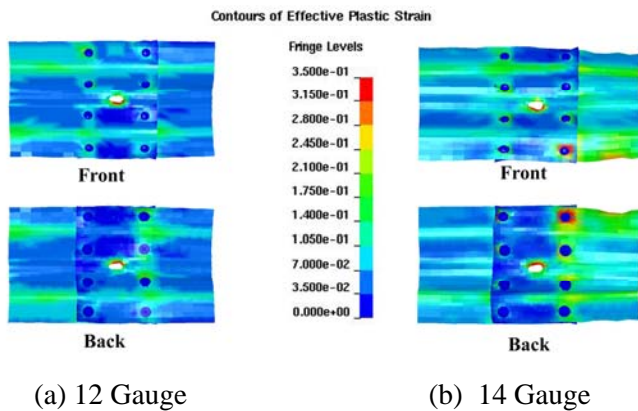


Figure 11 -: Plastic strains at the splice after impact showing higher stains in the 14 gauge rail.

Post and Blockout Gap

The analysis of design features also included addressing the concern that over time the wood blockout would shrink, creating a gap between the post and the blockout. This gap, it was thought, might undermine the benefits of routing blockouts by making it easier for the blockout to rotate. A 5mm gap, about half the depth of the routing, was modeled to reflect this condition. Figure 12 compares yaw angles between simulations run with and without the blockout gap. Figure 13 compares peak roll angles for simulations run with and without the blockout gap. The similarities of the curves suggest that such gaps will not detract from barrier performance.

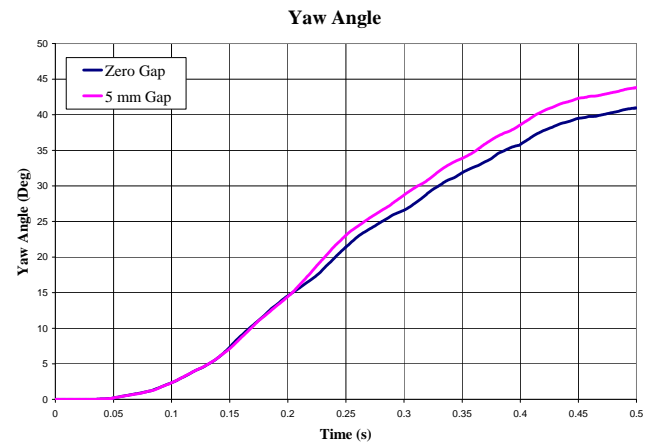


Figure 12 - Comparison of yaw angles for gap versus no gap conditions.

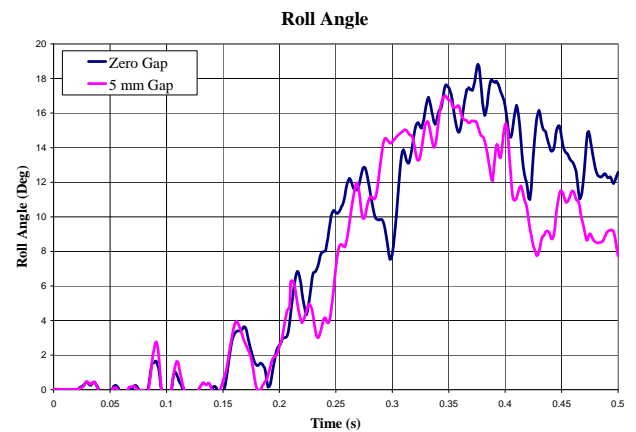


Figure 13 - Comparison of roll angles for gap versus no gap conditions.

Summary & Conclusions:

This research was successful in:

- Developing a finite element model for the w-beam guardrail G4(1s) system.
- Validating the model against several full-scale crash tests to provide confidence in its application.
- Demonstrating use of the model to compare guardrail performance for variations in design features was demonstrated.
- Confirming that routed blockouts provided better performance. The concept of simply adding an additional bolt between the post and the blockout was shown to reduce rotation, but overall performance was poorer than with the routed blockout.
- Analyzing the effects of changing the gauge of the steel in the guardrail, showing that while the system would meet the requirements, the rail material was reaching its maximum strain capacity which could

lead to a failure over time due to corrosion or other damage..

- Comparing effect of the gap between the posts and the routed blockouts on system performance, and showing that a gap of 5mm or less would not detract from barrier performance.

Useful insights were derived from these efforts, and a new tool for the analysis of w-beam guardrail performance was developed.

References:

1. Ross, H. E., Sicking, D., and Zimmer, R. A., "Recommended Procedures for the Safety Performance Evaluation of Highway Features", NCHRP Report 350, Transportation Research Board, Washington D.C., 1993.
2. Buth, C.E., Menges, W.L., Ivey, D.L., and Williams, W.F., "W-Beam Guardrail" Proceedings of the 78th Annual Meeting Transportation Research Board, Paper No. 990871, Washington D.C., January 1999.
3. Polivka, K.A., Sicking, D.L., Rohde, J.R., Faller, R.K., and Holloway, J.C., "Crash Testing of Michigan's Type B (W-Beam) Guardrail System", Midwest Roadside Safety Facility, Report No. TRP-03-90-99, Nov 1999.
4. Polivka, K.A., Sicking, D.L., Rohde, J.R., Faller, R.K., and Holloway, J.C., "Crash Testing of Michigan's Type B (W-Beam) Guardrail System – Phase II", Midwest Roadside Safety Facility, Report No. TRP-03-104-00, October 2000.
5. Hallquist, J. O., LS-DYNA User's Manual, Livermore Software Technology Corporation, April 2003.
6. Eskandarian, A., Marzougui, D., and Bedewi, N., "Impact Finite Element Analysis of Slip-Base Sign Support Mechanism", ASCE Journal of Transportation Engineering, Vol. 126, No. 2, March 2000.
7. Marzougui, D., Bahouth, G., Eskandarian, A., Meczkowski, L., and Taylor, H., "Evaluation of Portable Concrete Barriers Using Finite Element Simulation", In Transportation Research Record 1720, TRB, Washington DC, 2000.
8. Marzougui, D., Meczkowski, L., Taylor, H. and Bedewi, N., "Sign support height analysis using finite element simulation", International Journal of Crashworthiness , Vol. 6, No. 1, 2001.
9. Belytschko, T., Lin, J., and Tsay, C.S., "Explicit algorithms for non-linear dynamics of shells," Computer Methods in Applied Mechanics and Engineering, 1984.
10. Marzougui, Mohan, & Kan; "Evaluation of Rail Height Effects on the Safety Performance of W-Beam Barriers," NCAC 2007-R-00x.
11. Whitworth H.A., Bendidi R., Marzougui D., and Reiss R., "Finite Element Modeling of the Crash Performance of Roadside Barriers", International Journal of Crashworthiness, Vol. 9, No. 1 2003.

For More Information:

See the NCAC Website (www.ncac.gwu.edu) for more information including:

- Documents from related efforts.
- Power point files providing and overview of the effort as well as the crash videos and animations
- Other NCAC information
- Information on other NCAC efforts

Or, contact:

- FHWA Roadside Safety Team
Dr. Ken Opiela, PE (Team Leader)
202-493-3371
kenneth.opiela@fhwa.dot.gov
- NCAC Staff
Dr. Steve Kan, Director
703-726-8511
cdkan@ncac.gwu.edu
Dr. Dhafer Marzougui
703-726-8532
dmarzoug@ncac.gwu.edu

This Technical Summary was produced under Cooperative Agreement DTFH61-02-X-00076 "Operation & Maintenance of the FHWA/NHTSA National Crash Analysis Center" between FHWA and George Washington University.

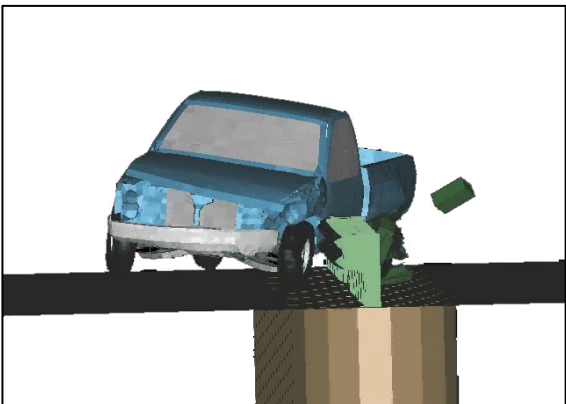
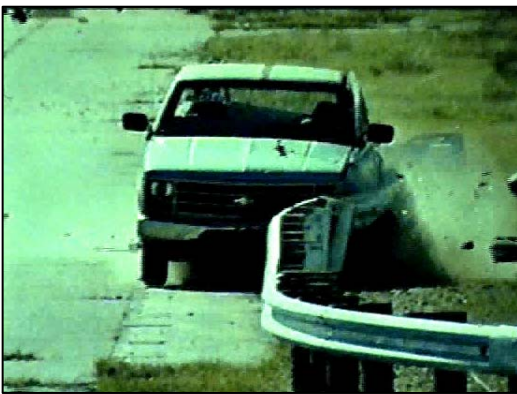
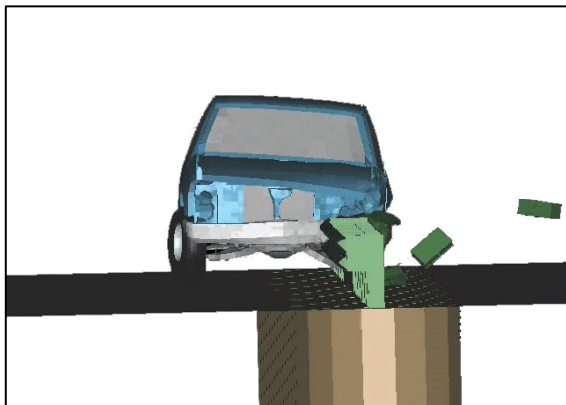
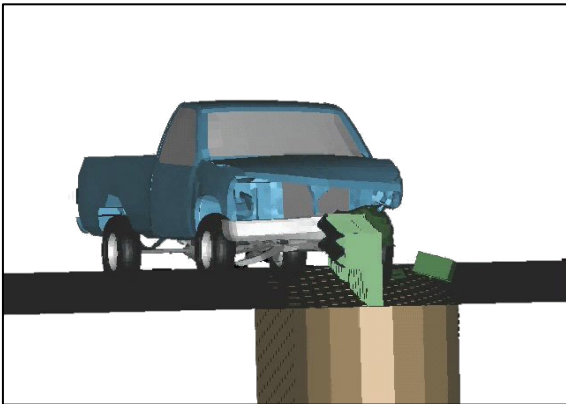
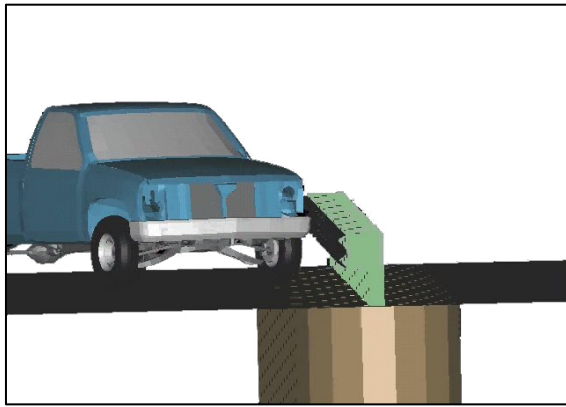


Figure 8: Simulation versus full-scale crash test view for NCHRP 350 Test 3-11